Electronic Supplementary Information for

A DFT Study on Photoinduced Surface Catalytic Coupling Reactions on Nanostructured Silver Surfaces: Selective Formation of Azobenzene Derivatives from *para*-Substituted Nitrobenzene and Aniline

Liu-Bin Zhao, Yi-Fan Huang, Xiu-Min Liu, Jason R. Anema,
De-Yin Wu,* Bin Ren, and Zhong-Qun Tian

(1) Testing reliability of theoretical methods

To elucidate the reliability of the present theoretical methods, we presented the optimized structure and simulated Raman spectra of nitrobenzene (NB), aniline (AN), and azobenzene (AB) as shown in Figure S1. Table S1 presents the bond distances of NB, AN, and AB calculated by using different functionals.

Compared with the data of the NB molecule from the gas-phase microwave spectroscopy and the gas electron diffraction (GED), hybrid functional B3LYP method is better than pure functionals PW91PW91 and BP86 methods in predicting N-O interaction. The N-O bond length calculated by B3LYP is 1.225 Å, in good accordance with both microwave and GED measured value of 1.227 Å.[1-2] The N-O bond length predicted by PW91PW91 and BP86 methods are 1.236 and 1.239 Å, respectively. Therefore these two functionals underestimate N-O bond strength. All the C-N bond lengths calculated from the three functionals fall in between the microwave and GED data.

Underestimating the N-O bond distance by BP86 and PW91PW91 leads to a bad description of the N-O stretching vibration. The calculated frequencies of the N-O symmetric stretching mode by BP86 and PW91PW91 are 1296 and 1307 cm^{-1}, respectively, which are obviously lower than the experimental value at 1347 cm^{-1}.[3] On the other hand, the B3LYP frequency is 1346 cm^{-1} very close to experimental data, indicating the B3LYP method is good at predicting the N-O bond strength and its related vibrations.

All the three functionals give similar results in predicting the structures of AN as well as its vibrational spectra. Both the C-N band and the C-C bands are quite close to gas-phase microwave data. At the same time, the simulated Raman spectra of aniline exactly reproduce Tian's experiment result.[4] This further demonstrates that all three functionals used are good at describing aromatic amines.

As compared with the data of AB from the X-ray crystal structure and the GED, it is clear that the PW91PW91, BP86, and B3LYP functionals predict well the C-N bond distance. On the other hand, only the PW91PW91 and BP86 functionals predicted well the N=N bond distance. PW91PW91 and BP86 gave the N=N bond distances of 1.267 and 1.271 Å, respectively, in good agreement with the value of 1.268 Å measured by GED.[5] However, the B3LYP bond distance is obviously shorter than the experimental data. This indicates that the hybrid DFT approaches may overestimate the bonding strength of the azo N=N bond in AB compounds.

PW91PW91 and BP86 functionals also led to the best simulated Raman spectra of the AB molecule[6] (see Figure S1). The N=N stretching mode calculated by BP86 and PW91PW91 are 1409 and 1419 cm^{-1}, respectively. They are close to the experimental measurement of 1441 cm^{-1}.[6] B3LYP method overestimates N=N bond strength, which predicts the frequency of N=N stretching at 1520 cm^{-1}. The frequencies of normal modes of AB are calculated well by the PW91PW91 method followed by the BP86 method.[7-8]

From the above discussion, we can conclude that B3LYP method is good at predicting the N-O bond while BP86 and PW91PW91 functionals are good at describe the N=N bond. All the three methods can describe the C-N bond in aniline and azobenzene well. Accurate prediction of the equilibrium structure is very important to theoretically simulate the molecular vibrational spectra.

Table S1 Comparison of Calculated and Measured Bond Distances (Å) of NB, AN, and AB Calculated by Using Different Theoretical Methods.

Nitrobenzene	B3LYP	PW91PW91	BP86	Microwave[1]	X-ray	GED[2]
C-N	1.481	1.485	1.489	1.492		1.474
N-O	1.225	1.236	1.239	1.227		1.228
C1-C2	1.391	1.397	1.400	1.375		1.387
C2-C3	1.391	1.396	1.399	1.403		1.415
C3-C4	1.395	1.400	1.403	1.396		1.393
Aniline	B3LYP	PW91PW91	BP86	Microwave[9]	X-ray[10]	GED[11]
C-N	1.398	1.398	1.402	1.402	1.398	1.406
C1-C2	1.403	1.409	1.399	1.397	1.404	1.403
C2-C3	1.391	1.396	1.399	1.394	1.380	1.393
C3-C4	1.395	1.399	1.402	1.396	1.386	1.396
Azobenzene	B3LYP	PW91PW91	BP86	Microwave	X-ray[12]	GED[5]
N-N	1.252	1.267	1.271		1.247	1.260
N-C	1.419	1.417	1.421		1.428	1.427
C3-C4	1.404	1.410	1.413		1.387	1.405
C4-C5	1.388	1.392	1.395		1.384	1.393
C5-C6	1.399	1.404	1.407		1.382	1.402
C6-C7	1.393	1.399	1.402		1.391	1.397

C7-C8	1.392	1.396	1.399		1.384	1.396

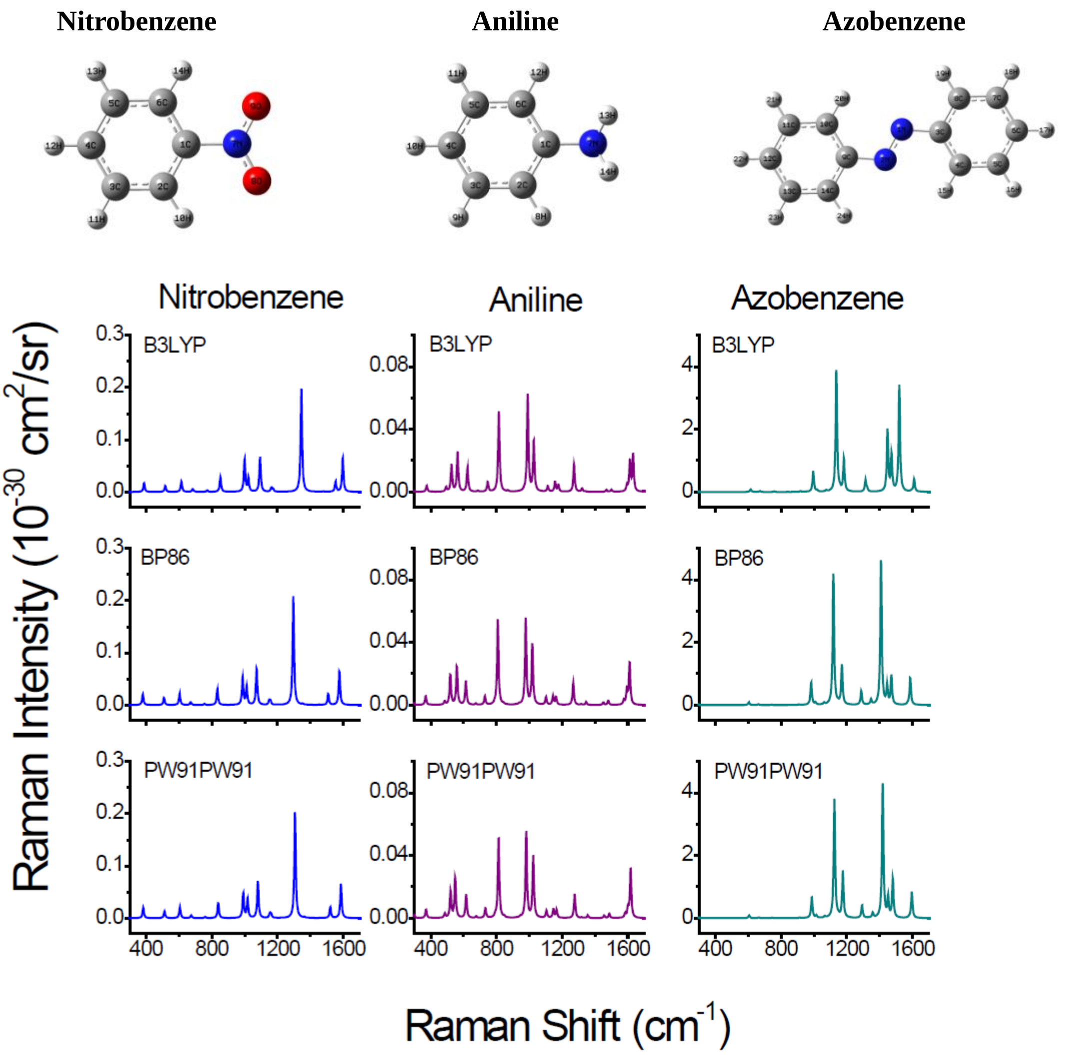

Fig. S1 Simulated normal Raman spectra of NB (left), AN (middle), and AB (right) using B3LYP, BP86 and PW91PW91 combining with the basis set of 6-311+G**. An excitation wavelength of 632.8 nm and a line width of 10 cm^{-1} were used in the simulated Raman spectra.

---

(2) Simulated Raman spectra with different clusters

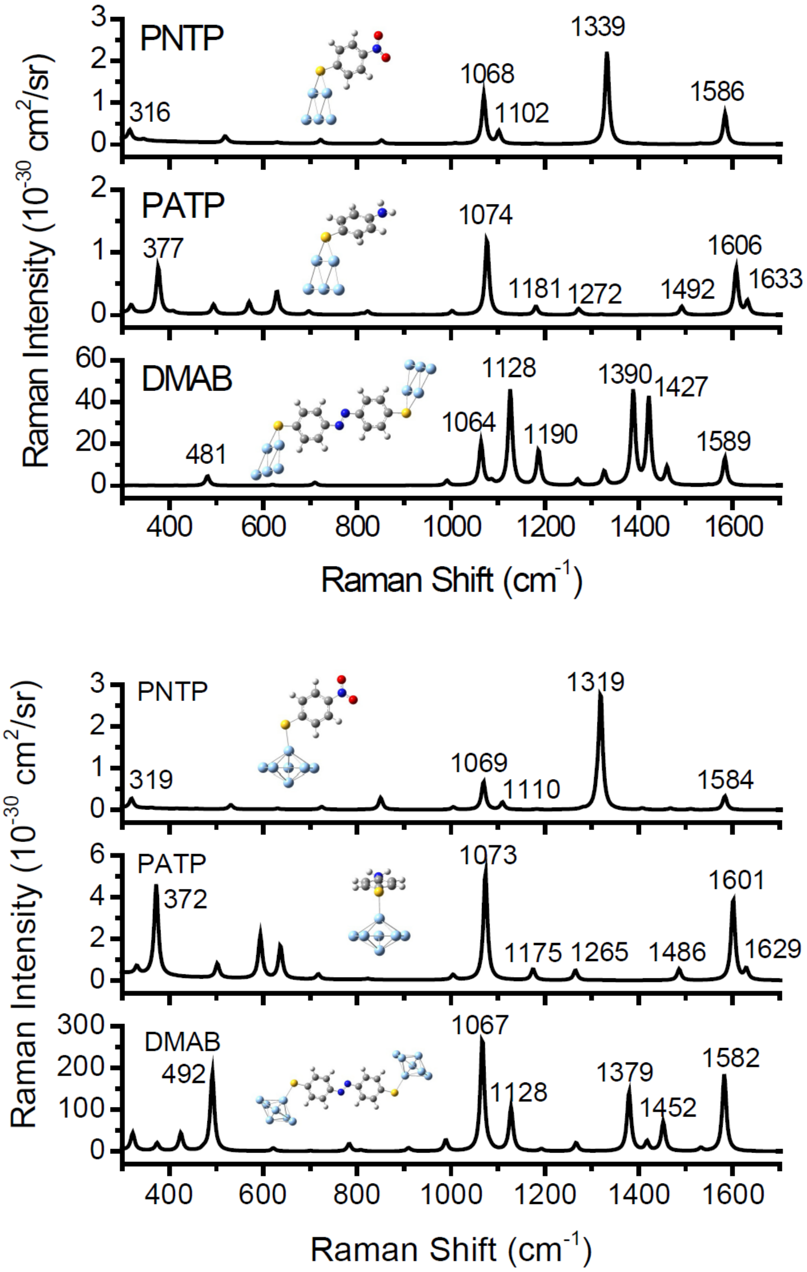

Fig. S2 Simulated normal Raman spectra of Ag_m-PNTP, Ag_m-PATP (B3LYP/6-311+G(d,p)/LANL2DZ) and Ag_m-DMAB-Ag_m (PW91PW91/6-311+G(d, p)/LANL2DZ) (m = 5, 7). An excitation wavelength of 632.8 nm and a line width of 10 cm^{-1} were used in the simulated Raman spectra.

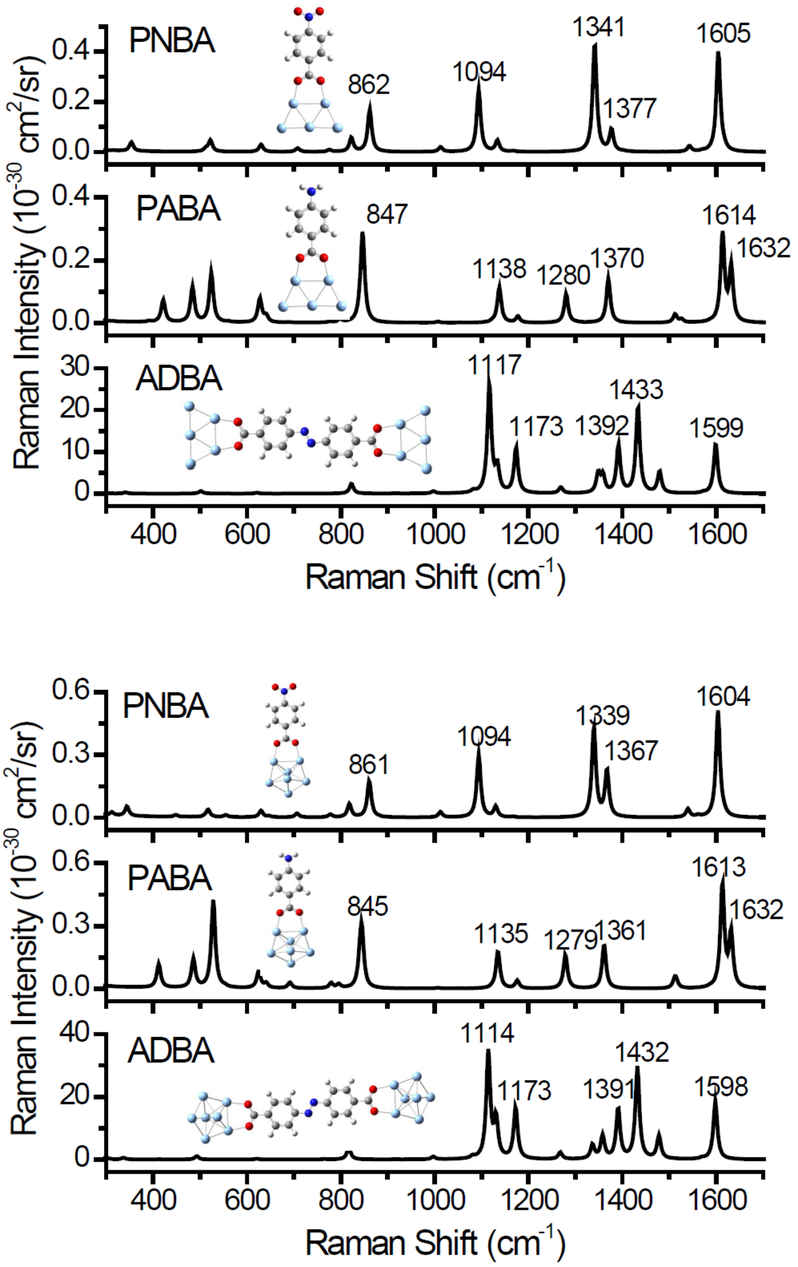

Fig. S3 Simulated normal Raman spectra of Ag$_m$-PNBA, Ag$_m$-PABA (B3LYP/6-311+G(d,p)/LANL2DZ) and Ag$_m$-ADBA-Ag$_m$ (PW91PW91/6-311+G(d, p)/LANL2DZ) (m = 5, 7). An excitation wavelength of 632.8 nm and a line width of 10 cm^{-1} were used in the simulated Raman spectra.

---

(3) Vibrational analysis

Table S2 Comparison of experimental Raman and SERS spectra with theoretical harmonic frequencies (cm^{-1}) and Raman scattering activity ($Å^4$/amu) of PNBA calculated at the B3LYP/6-311+G(d,p) level. Vibrational assignment is based on the potential energy distribution.

NR		SERS		Assignments
Experiment[13]	Calculation	Experiment[13]	Calculation	
1620 (w)	1616 (8.29)		1617 (10.21)	$\upsilon_{as}CO_2$
1600 (m)	1604 (229.54)	1600 (s)	1604 (687.94)	$\upsilon C{-}C$
1525 (w)	1536 (25.04)		1539 (27.86)	$\upsilon_{as}NO_2$
1395 (m)	1384 (92.96)	1395 (m)	1370 (310.32)	$\upsilon_{s}CO_2$
1350 (s)	1341 (247.74)	1355 (s)	1339 (410.75)	$\upsilon_{s}NO_2$
1145 (w)	1127 (14.72)		1130 (42.35)	$\upsilon C{-}CO_2$, βCH
1115 (m)	1093 (92.83)	1115 (m)	1094 (218.79)	$\upsilon C{-}NO_2$, βCH
875 (m)	863 (52.85)	875 (m)	861 (80.77)	βNO_2
805 (w)	832 (6.30)	835 (w)	820 (23.75)	βCO_2

Table S3 Comparison of experimental Raman and SERS spectra with theoretical harmonic frequencies (cm^{-1}) and Raman scattering activity ($Å^4$/amu) of PABA calculated at the B3LYP/6-311+G(d,p) level. Vibrational assignment is based on the potential energy distribution.

NR		SERS		Assignments
Experiment[14]	Calculation	Experiment[14]	Calculation	
	1631 (80.14)		1632 (279.42)	$\delta\mathrm{NH}_2$
1605 (s)	1613 (119.81)	1604(s)	1613 (523.48)	υC–C
1517 (w)	1516 (12.05)	1517(w)	1512 (54.61)	$\upsilon_{as}\mathrm{CO}_2$
1382 (s)	1380 (104.63)	1373(s)	1365 (322.11)	$\upsilon_{s}\mathrm{CO}_2$
1279 (w)	1273 (31.25)	1253(w)	1278 (118.51)	υC–N
1178 (w)	1173 (5.39)	1178(w)	1176 (25.19)	βCH
1139 (m)	1129 (28.50)	1139(w)	1135 (111.81)	$\upsilon\mathrm{C{-}CO}_2$, βCH
855 (s)	851 (71.49)	855(w)	845 (30.34)	νC–C
		793(w)	796 (7.70)	$\beta\mathrm{CO}_2$
638 (w)	641 (6.41)	638(w)	627 (23.86)	α_{as}ring

Table S4 Characteristic vibrational Raman frequencies and their potential energy distribution of azobenzene and its derivatives calculated by PW91PW91/6-311+G(d,p)

Molecule	Characteristic Vibrational Frequency and PED			
Azobenzene	1125 νC–N(25) βC–H(43)	1176 νC–N(22) βC–H(44)	1419 νN=N(44) νC–C(19) βC–H(34)	1481 νN=N(38) νC–C(25) βC–H(32)
–SH	1129 νC–N(23) βC–H(49)	1192 νC–N(24) βC–H(42)	1392 νN=N(38) νC–C(38) βC–H(20)	1428 νN=N(25) νC–C(33) βC–H(31)
–COOH	1121 νC–N(25) βC–H(42)	1182 νC–N(16) βC–H(36)	1397 νN=N(19) νC–C(52) βC–H(19)	1435 νN=N(37) νC–C(25) βC–H(28)
$-NH_2$	1129 νC–N(19) βC–H(57)	1193 νC–N(29) βC–H(37)	1399 νN=N(62) νC–C(21) βC–H(12)	1451 νN=N(10) νC–C(46) βC–H(25)
$-NO_2$	1124 νC–N(23) βC–H(42)	1172 νC–N(24) βC–H(38)	1394 νN=N(21) νC–C(48) βC–H(24)	1436 νN=N(22) νC–C(29) βC–H(37)
–OH	1123 νC–N(17) βC–H(57)	1181 νC–N(31) βC–H(34)	1405 νN=N(50) νC–C(25) βC–H(18)	1455 νN=N(20) νC–C(36) βC–H(20)
–CN	1123 νC–N(27) βC–H(42)	1181 νC–N(19) βC–H(47)	1397 νN=N(23) νC–C(49) βC–H(26)	1433 νN=N(36) νC–C(27) βC–H(27)

(4) Pre-resonance Raman Spectra

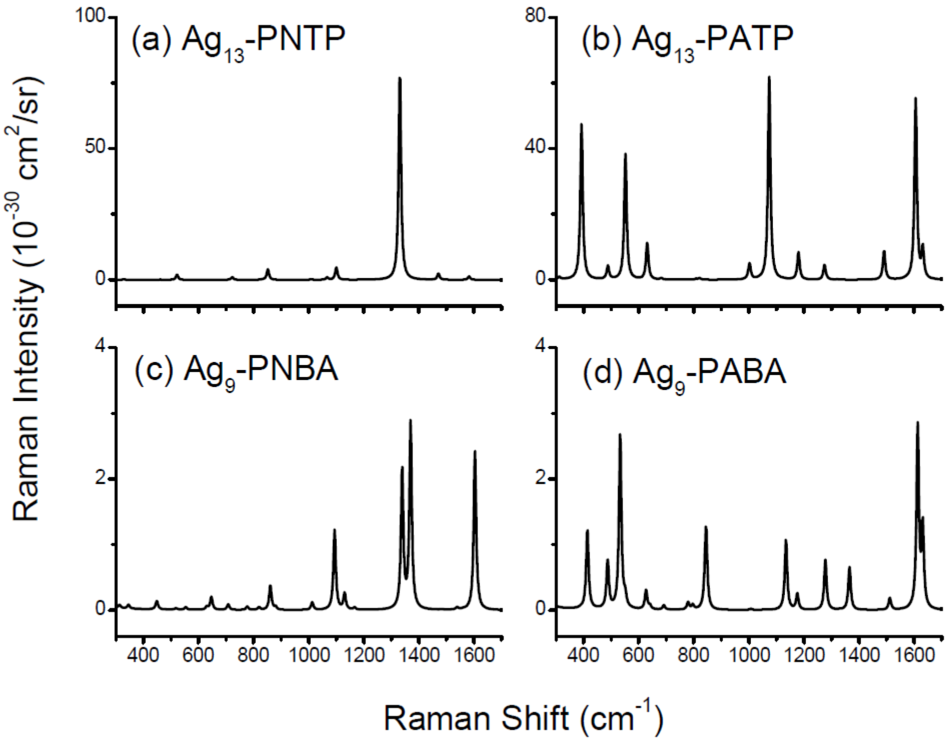

Fig. S4 Simulated pre-resonance Raman spectra of (a) Ag_{13}-PNTP, (b) Ag_{13}-PATP, (a) Ag_9-PNBA, and (d) Ag_9-PABA at B3LYP/6-311+G(d, p)/LAN2DZ. The incident wavelength was chosen to have energy gaps of 0.1 eV lower than the low-lying CT excited state.

(5) Molecular Orbitals and TD-DFT

Table S5 Molecular Orbitals and Low-lying Charge Transfer Transitions of Ag_{13}-PNTP complex Calculated at B3LYP/6-311+G(d,p) level.

Occupied		Unoccupied	
HOMO (163)	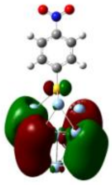	LUMO (164)	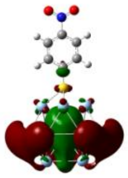
HOMO-1 (162)	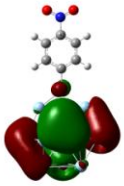	LUMO+1 (165)	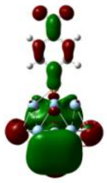
HOMO-2 (161)	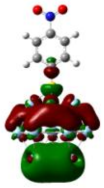	LUMO+2 (166)	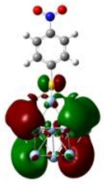
HOMO-3 (160)	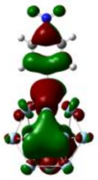	LUMO+3 (167)	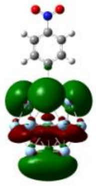
HOMO-4 (159)	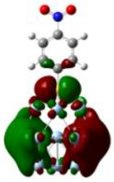	LUMO+4 (168)	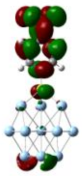
HOMO-5 (158)	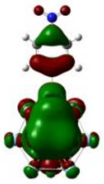	LUMO+5 (169)	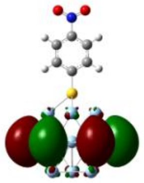

Excited State 19: Singlet-A 1.7273 eV 717.81 nm f=0.0001
162A ->168A 0.10103
163A ->165A 0.11302
163A ->168A 0.68265
162B ->168B 0.10103
163B ->165B 0.11302
163B ->168B 0.68265
Excited State 20: Singlet-A 1.7643 eV 702.73 nm f=0.0508
162A ->165A 0.11909
162A ->168A 0.67641

162B ->165B 0.11909
162B ->168B 0.67641

Table S6 Molecular Orbitals and Low-lying Charge Transfer Transitions of Ag_{13}-PATP complex Calculated at B3LYP/6-311+G(d,p) level.

Occupied		Unoccupied	
HOMO (156)	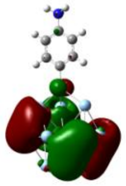	LUMO (157)	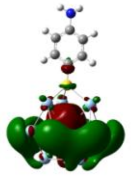
HOMO-1 (155)	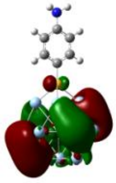	LUMO+1 (158)	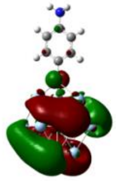
HOMO-2 (154)	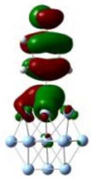	LUMO+2 (159)	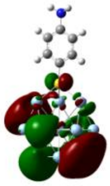
HOMO-3 (153)		LUMO+3 (160)	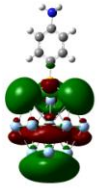
HOMO-4 (152)	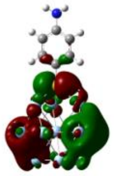	LUMO+4 (161)	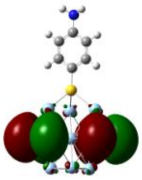
HOMO-5 (151)	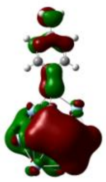	LUMO+5 (162)	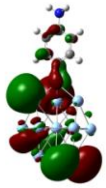

Excited State 24: Singlet-A 2.2823 eV 543.25 nm f=0.0006
154A ->157A 0.68392
155A ->161A 0.14613
154B ->157B 0.68392
155B ->161B 0.14613
Excited State 27: Singlet-A 2.3873 eV 519.35 nm f=0.0034
153A ->157A 0.67551
154A ->158A -0.11241

```
      153B ->157B        0.67551
      154B ->158B       -0.11241
```

Table S7 Molecular Orbitals and Low-lying Charge Transfer Transitions of Ag$_9$-PNBA complex Calculated at B3LYP/6-311+G(d,p) level.

Occupied		Unoccupied	
HOMO (128)		LUMO (129)	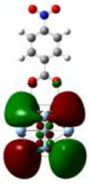
HOMO-1 (127)	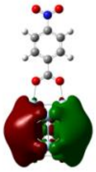	LUMO+1 (130)	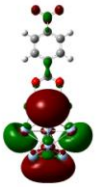
HOMO-2 (126)		LUMO+2 (131)	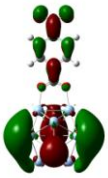
HOMO-3 (125)		LUMO+3 (132)	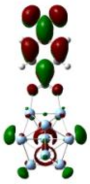
HOMO-4 (124)	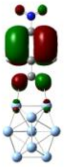	LUMO+4 (133)	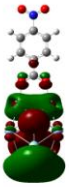
HOMO-5 (123)		LUMO+5 (134)	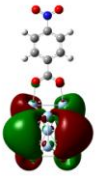

```
 Excited State   8:   Singlet-A      2.0012 eV  619.54 nm  f=0.0031
      127A ->129A       -0.13984
      128A ->130A       -0.13782
      128A ->131A        0.58810
      128A ->132A        0.31766
      127B ->129B       -0.13984
      128B ->130B       -0.13782
      128B ->131B        0.58810
```

128B ->132B 0.31766
Excited State 14: Singlet -A 2.2943 eV 540.40 nm f=0.0072
127A ->129A -0.10814
128A ->131A -0.32869
128A ->132A 0.60620
127B ->129B -0.10814
128B ->131B -0.32869
128B ->132B 0.60620

Table S8 Molecular Orbitals and Low-lying Charge Transfer Transitions of Ag_9-PABA complex Calculated at B3LYP/6-311+G(d,p) level.

Occupied		Unoccupied	
HOMO (121)		LUMO (122)	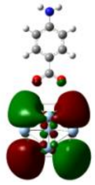
HOMO-1 (120)	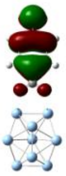	LUMO+1 (123)	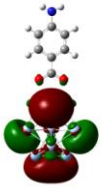
HOMO-2 (119)		LUMO+2 (124)	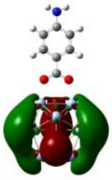
HOMO-3 (118)		LUMO+3 (125)	
HOMO-4 (117)	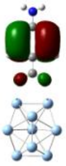	LUMO+4 (126)	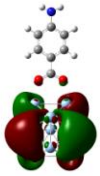
HOMO-5 (116)		LUMO+5 (127)	

Excited State 11: Singlet -A 2.2072 eV 561.73 nm f=0.0001
120A ->122A 0.70166

```
      120B ->122B          0.70166
 Excited State   21:   Singlet -A        2.6403 eV  469.59 nm  f=0.0274
      118A ->123A          0.12087
      120A ->123A          0.67576
      121A ->125A         -0.12993
      118B ->123B          0.12087
      120B ->123B          0.67576
      121B ->125B         -0.12993
```

---

1 V. A. Shlyapochnikov, L. S. Khaikin, O. E. Grikina, C. W. Bock and L. V. Vilkov, *J. Mol. Struct.*, 1994, **326**, 1-16.

2 O. Dorofeeva, Y. Vishnevskiy, N. Vogt, J. Vogt, L. Khristenko, S. Krasnoshchekov, I. Shishkov, I. Hargittai and L. Vilkov, *Struct. Chem.*, 2007, **18**, 739-753.

3 J. Clarkson and W. Ewen Smith, *J. Mol. Struct.*, 2003, **655**, 413-422.

4 Z. Q. Tian, L. C. Lei and X. B. Jing, *Acta Physico-Chimica Sinica*, 1988, **4**, 458-460.

5 T. Tsuji, H. Takashima, H. Takeuchi, T. Egawa and S. Konaka, *J. Phys. Chem. A*, 2001, **105**, 9347-9353.

6 Y.-C. Liu and R. L. McCreery, *Anal. Chem.*, 1997, **69**, 2091-2097.

7 D. Y. Wu, X. M. Liu, Y. F. Huang, B. Ren, X. Xu and Z. Q. Tian, *J. Phys. Chem. C*, 2009, **113**, 18212-18222.

8 N. Kurita, S. Tanaka and S. Itoh, *J. Phys. Chem. A*, 2000, **104**, 8114-8120.

9 D. G. Lister, J. K. Tyler, J. H. Høg and N. W. Larsen, *J. Mol. Struct.*, 1974, **23**, 253-264.

10 M. Fukuyo, K. Hirotsu and T. Higuchi, *Acta Cryst.*, 1982, **B38**, 640-643.

11 G. Schultz, G. Portalone, F. Ramondo, A. Domenicano and I. Hargittai, *Struct. Chem.*, 1996, **7**, 59-71.

12 J. A. Bouwstra, A. Schouten and J. Kroon, *Acta Cryst.*, 1983, **C39**, 1121-1123.

13 P. G. Roth, R. S. Venkatachalam and F. J. Boerio, *J. Chem. Phys.*, 1986, **85**, 1150-1155.

14 H. Park, S. B. Lee, K. Kim and M. S. Kim, *J. Phys. Chem.*, 1990, **94**, 7576-7580.